Bulletin of the Seismological Society of America, Vol. 73, No. 2, pp. 537–551, April 1983

SOURCE PROCESSES OF LARGE EARTHQUAKES ALONG THE XIANSHUIHE FAULT IN SOUTHWESTERN CHINA

BY HUILAN ZHOU, HSUI-LIN LIU, AND HIROO KANAMORI

ABSTRACT

The Xianshuihe fault is one of the most active faults in southwestern China. Recently, three large earthquakes occurred along it in 1967 (M_S = 6.1), 1973 (M_S = 7.5), and 1981 (M_S = 6.8).

The 1981 event occurred near the central portion of the fault zone. Modeling of the body and surface waves indicates pure left-lateral strike-slip motion on a vertical fault striking N40°W consistent with the surface trend of the Xianshuihe fault. Two major ruptures are suggested for this source, with a total moment of 1.3×10^{26} dyne-cm. The 1973 event occurred about 65 km northwest of the 1981 event and ruptured about 90 km bilaterally along the fault. The body-wave synthetics indicate three main ruptures during faulting within 43 sec, with a total moment of 1.8×10^{27} dyne-cm. The mechanisms are similar to the 1981 event, and the average slip is determined to be 3.8 m. The largest aftershock (M_S = 5.9) occurred 1 day after the main event with a normal-fault mechanism striking almost perpendicular to the surface breakage. The 1967 event occurred at the northwestern end of the fault zone, with a strike of N65°E. It had a nearly normal-fault mechanism with a seismic moment of 4.5×10^{25} dyne-cm. The largest aftershock (M_S = 5.1) occurred 7 hr later with a similar focal mechanism.

The primary faulting along the Xianshuihe fault is left-lateral strike-slip, but the normal faulting with strike direction about perpendicular to the Xianshuihe fault trace is common, especially in the northwestern segment. The faulting pattern in this region is consistent with the regional stress field caused by the India-Tibet collision. The normal event which is not on the major fault seems to have more frequent foreshocks and aftershocks than those on the main fault.

INTRODUCTION

Yunnan and Sichuan provinces, shown in Figure 1a, are among the most seismically active regions in southwestern China. It is generally believed that the tectonic stress field in this area is controlled by the India-Tibet collision, which is manifested by a bell-shaped collision zone pointing northeastward toward the center of this area (Molnar and Tapponnier, 1975). The regional structural features as well as the morphology are strongly influenced by this currently active collision. In the northeastern part of this area, the Xianshuihe, Anninghe, and Xiaojiang faults form an active left-lateral fault system striking northwest to north (Figure 1a). In the central part, the Honghe fault (Red River fault) extends from northwest to southeast, with clear right-lateral motion in its southern segment, which is adjacent to the left-lateral Xiaojiang fault (Figure 1a) (Kan *et al.*, 1977). Most of the large earthquakes with $M_S > 7$ in this area have occurred along these major fault systems.

The Xianshuihe fault, which has also been called the Kangding fault (e.g., Lee, 1948; Tapponnier and Molnar, 1977), is recognized as the most active fault zone in the area, since there have been three $M_S > 7$ earthquakes on it in the past 60 yr: the 1923 Daofu event (M_S = 7.3); the 1955 Kangding event (M_S = 7.5); and the 1973 Luhuo event (M_S = 7.5). The distribution of the earthquakes with $M_S > 6.0$ in this area is shown in Figure 1b. The earthquake origin times and locations are listed in Table 1. The Xianshuihe fault extends from Ganzi southeast to Kangding with a

total length of about 300 km. The 6 February 1973 earthquake with M_S = 7.5 is located about 20 km northwest of the 1923 event, which has an estimated M_S = 7.3. The surface rupture of the 6 February 1973 event is about 90 km long (Tang *et al.*, 1976). The faulting of both the 1955 and 1973 events is left-lateral (Kan *et al.*, 1977).

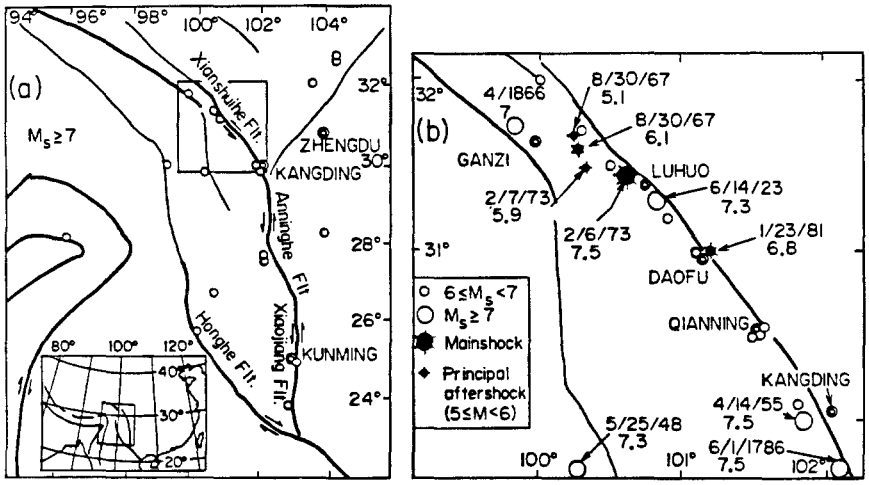

FIG. 1. (a) The major fault systems in southwestern China. The open circles are the events with M_S greater than 7.0 (780 B.C. to 1981). The magnitude of historical event is from *Catalogue of Strong Earthquakes in China* estimated by using an empirical relationship between magnitude and epicentral intensity. (b) The Xianshuihe fault and its associated earthquakes [the *boxed area* in (a)]. The solid dots are the three main shocks and two major aftershocks studied in this paper.

TABLE 1

EARTHQUAKES ALONG XIANSHUIHE FAULT

Event Date	Location		M_S CHINA	M_S USGS
	°N	°E		
1 June 1786	29.7	102.1	7.5	
7 September 1792	30.5	101.5	6	
15 May 1793	30.5	101.5	6	
27 September 1811	31.7	100.3	6	
00 April 1866	31.7	99.8	7	
29 August 1893	30.5	101.5	6.8	
30 August 1904	31.2	100.9	6	
29 May 1919	31.5	100.5	6.3	
25 August 1919	32.0	100.0	6.3	
24 March 1923	31.3	100.8	7.3	
14 June 1923	31.0	101.1	6.5	
6 March 1932	30.1	101.8	6	
14 April 1955	30.0	101.8	7.5	
30 August 1967*	31.6	100.3	6.8	6.1
30 August 1967*	31.7	100.3	6.0	5.1
6 February 1973*	31.4	100.6	7.9	7.5
7 February 1973*	31.5	100.3	6.0	5.9
23 January 1981*	31.0	101.2	6.9	6.8

* Events studied in this paper.

Photographs and descriptions by Heim (1934) of the 100-km-long fault ruture in 1923 strongly suggest left-lateral movement at that time because of the en-echelon fractures pattern. Furthermore, Heim's photographs of sag ponds and rift topography leave little doubt that the fault has a history of repeated late-Quaternary displacements.

TABLE 2

TELESEISMIC STATIONS USED IN THIS STUDY*

Station	Distance (°)	Azimuth (°)	Phases Used
	Event 30 August 1967 Main Shock		
BUL	85.8	243.4	*P*
COP	63.4	321.1	*P*
GUA	44.6	103.2	*P*
HNR	70.1	115.2	*P*
JER	54.6	288.9	*P*
KTG	70.3	342.0	*P*
LON	93.3	27.4	*P*
MUN	65.0	165.3	*P*
NOR	62.7	352.0	*P*
PRE	89.3	239.1	*P*
STU	67.6	314.3	*P*
TAU	85.8	147.0	*P*
TOL	80.2	311.4	*P*
	Event 30 August 1967 Principal Aftershock		
IST	56.7	301.1	*P*
KEV	55.0	335.4	*P*
MSH	33.9	289.3	*P*
POO	27.2	247.7	*P*
RAB	60.9	115.9	*P*
UME	57.9	329.0	*P*
	Event 6 February 1973 Main Shock		
AAE	61.1		*P*, *R*3
ADE	75.1	41	*P*, *G*3
CAR	136.7	342.0	*R*3, *G*3
COL	70.7	24.8	*P*, *G*3
COP	63.7	321.0	*G*3
GUA	44.5	103.0	*P*, *R*, *G*2
IST	57.0	301.4	*P*
JER	54.8	289.0	*R*3
LEM	38.5	168.4	*P*
MSH	34.1	289.8	*P*, *R*2, *R*3
NAI	68.3	254.6	*P*
RAB	60.6	115.8	*P*, *G*3
STU	67.9	314.6	*P*, *G*3
TAB	44.4	294.2	*R*3, *G*3
	Event 7 February Principal Aftershock		
AAE	61.1	263.2	*P*
ADE	75.3	148.0	*P*
COL	70.5	25.3	*P*
GUA	44.6	102.9	*P*
MSH	34.0	289.4	*P*
MUN	64.9	165.1	*P*
NAI	68.3	254.2	*P*
RAB	60.8	115.8	*P*
TAB	44.3	294.0	*p*
	Event 23 January 1981 Main Shock		
ANMO	109.5	23.7	*R*1, *G*1
ANTO	55.2	299.5	*P*, *R*1, *G*1
BCAO	81.3	270.1	*P*, *R*1, *G*1
CTAO	66.8	133.4	*P*, *R*1, *G*1

TABLE 2—*Continued*

Station	Distance (°)	Azimuth (°)	Phases Used
GRFO	67.0	315.2	*P*, *R*1, *G*1
GUMO	43.7	103.2	*R*1, *G*1
KONO	64.6	325.9	*P*, *R*1, *G*1
MAJO	69.5	270.7	*P*, *R*1, *G*1
NWAO	65.3	165.0	*P*, *R*1, *G*1
SNZO	98.9	132.8	*R*1, *G*1
AAE	61.7	263.5	*P*
MAT	31.3	69.5	*P*
MUN	64.2	165.7	*P*
NAI	68.8	255.1	*P*
RAB	59.9	116.2	*P*

* The stations used for first motion are not listed.

In addition to the 1973 event, an event with $M_S = 6.1$ occurred on 30 August 1967 near Ganzi and a $M_S = 6.8$ event occurred on 23 January 1981, near Daofu. Good quality seismological data are available for these three events and two major aftershocks (for the 1967 and 1973 events), which are introduced as solid dots in Figure 1b. In this paper, we report the results of our study of the radiated waveforms in an attempt to understand the earthquake source processes along the Xianshuihe fault.

Data Analysis

We analyze mainly teleseismic long-period body waves recorded at the World-Wide Standardized Seismograph Network (WWSSN) and the Seismic Research Observatory (SRO) stations at teleseismic distance between 30° and 90°. The body waves can be expressed as the source terms convolved with the earth filter and the instrument response. For a half-space structure, the vertical seismograms can be expressed as a sum of the *P*, *pP*, and *sP* phases with proper time lags, which are determined by the source depth. By trial-and-error procedure, we resolve the source term, which includes the fault parameters and the far-field source time function (e.g., Kanamori and Stewart, 1976). The surface waves are also used to determine the source parameters of the 1973 and 1981 events. For the 1973 main shock, we use the body-wave mechanism to generate the surface-wave synthetics and estimate the surface-wave moment. For the 1981 event, we use SRO long-period surface waves (200 sec) and determine the source mechanism using the method described by Kanamori and Given (1981). Table 2 lists all the stations and wave types used in this study. The source parameters determined by the available data will be described in the following.

The 1967 main shock. The 30 August 1967 ($M_S = 6.1$) earthquake is located to the northwest of Luhuo. The computed epicenter is about 10 km off the major surface trace of the Xianshuihe fault (see Figure 1b). The first-motion data indicate a normal-fault mechanism with a strike oriented northeasterly as shown in Figure 2. Both the observed teleseismic *P* waves (vertical component) and the best-matched synthetics are shown in Figure 2. One of the nodal planes has a strike of 245°, dip of 45° (in the NW), and the slip angle on this plane is −70°. A trapezoidal source time function with a 2.5-sec total width matches the pulse width very well, and an average seismic moment of 4.5×10^{25} dyne-cm is obtained. The source depth of 8 km is used for the synthesis. The distribution evidence is available to determine the rupture plane. The distribution of the aftershocks projected on a plane perpendicular to the

likely to be the fault plane, but this interpretation is somewhat ambiguous. In the epicentral area, there are both northwest and southeast dipping faults striking to the NE, indicating a regional extension axis in NW-SE direction.

A major aftershock of the 1967 events. A major aftershock (M_S = 5.1) occurred 7

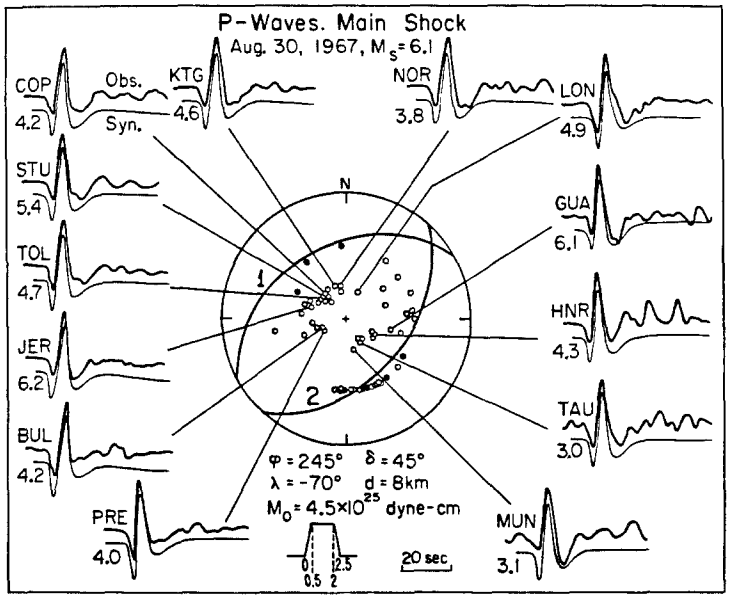

FIG. 2. The observed telesemismic *P* waves (vertical component) and synthetics for the 30 August 1967 main event. The first-motion data on the lower focal hemisphere are also shown (open circle: dilatation; closed circle: compression). Strike and dip of the nodal planes are: plane 1—ϕ = 245.0°, δ = 45.0°; plane 2—ϕ = 38.0°, δ = 48.0°.

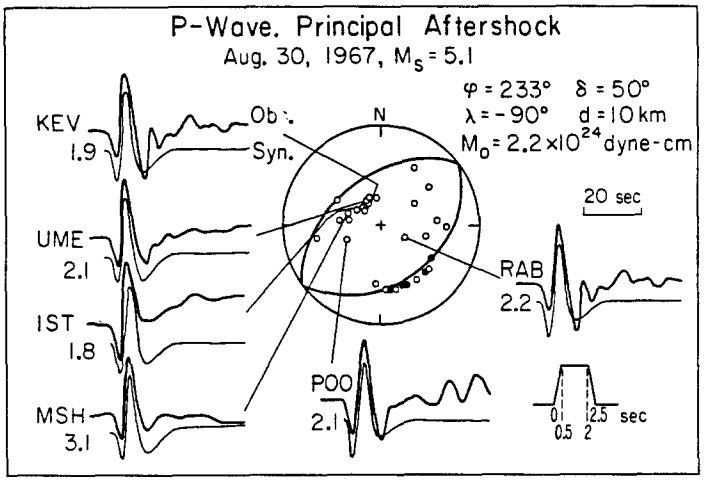

FIG. 3. The major aftershock (M_S = 5.1) of the 1967 event. Both observed and the best-matched synthetics are shown. Note that the first-motion data indicate a fault geometry similar to the main shock.

strike direction indicates that the nodal plane dipping to the northwest is more hr after the 1967 main event. As shown in Figure 3, the first-motion data indicate a mechanism similar to that of the main event. Only six teleseismic stations recorded clear vertical *P* waves, which are used to determine the source parameters here. The solution has a similar source orientation to that of the main shock [strike =

233°, dip = 50° (in the NW), and slip = −90°]. A trapezoidal far-field source time function with a 2.5-sec width and a seismic moment of 2.2×10^{24} dyne-cm can explain the observed waveforms when a source depth of 10 km is used.

The 1973 main shock. The earthquake of 6 February 1973 ($M_S = 7.5$) caused a 90-km-long surface rupture along the Xianshuihe fault (Tang *et al.*, 1976). The maximum left-lateral surface slip was about 3 m near Luhuo. The teleseismic *P* waves (vertical component) shown in Figure 4 indicate a complex feature of the earthquake source. The lower hemisphere projection of the first *P* motions shows a

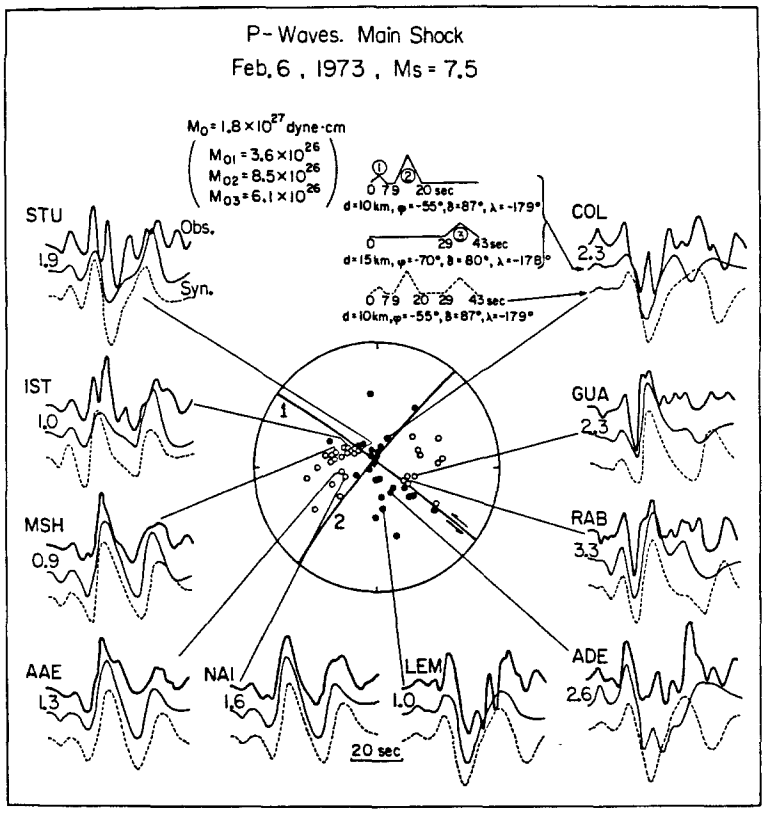

FIG. 4. The observed teleseismic *P* waves (vertical component) and the synthetics for the 6 February 1973 event. The solid *upper traces* are the observed seismograms. The *middle traces* are the synthetics for our preferred model which includes three events. The first and second events have the same fault geometry as indicated by the first-motion data shown in the figure. The third event has a different strike and dip direction. The *lower traces* (dashed lines) are the synthetics in which the three subevents have the same fault geometry as the first earthquake. The total moment is determined to be 1.8×10^{27} dyne-cm. Strike and dip angles of the nodal planes for the first and second events are: plane 1—$\phi = -55.0°$, $\delta = 87.0°$; plane 2—$\delta = 215.0°$, $\delta = 89.0°$. Strike and dip angles of the nodal planes for the third event are: plane 1—$\delta = -70.0°$, $\delta = 80.0°$; plane 2—$\phi = 200.0°$, $\delta = 88.0°$.

nearly pure strike-slip mechanism. The preferred source model obtained by a trial-and-error procedure comprises three events. The first two events have the same assumed source depth of 10 km and the same fault geometry, with strike = −55°, dip = 87° (in the NE), and slip = −179°, which is the same as the first-motion solution. The far-field source time history consists of two triangles, with 7- and 11-sec total duration, respectively. If the same mechanism is used for the third event, a slight mismatch occurs between the synthetics and the observed waveforms at stations COL, GUA, RAB, and ADE (dashed curve in Figure 4). The third event is

therefore given a slightly different source orientation (strike = −70°, dip = 80°, and slip = −178°) and source depth (15 km). This event occurred about 29 sec after the origin time and lasted about 14 sec, producing the long up-swing pulses at the end of the records shown in Figure 4. The synthetics for the sum of these three multiple sources are illustrated in the *middle traces* in Figure 4. The total moment is determined to be 1.8×10^{27} dyne-cm. In the first 30 sec of the records, the main contribution is from the second event, which has the seismic moment of about 8.5

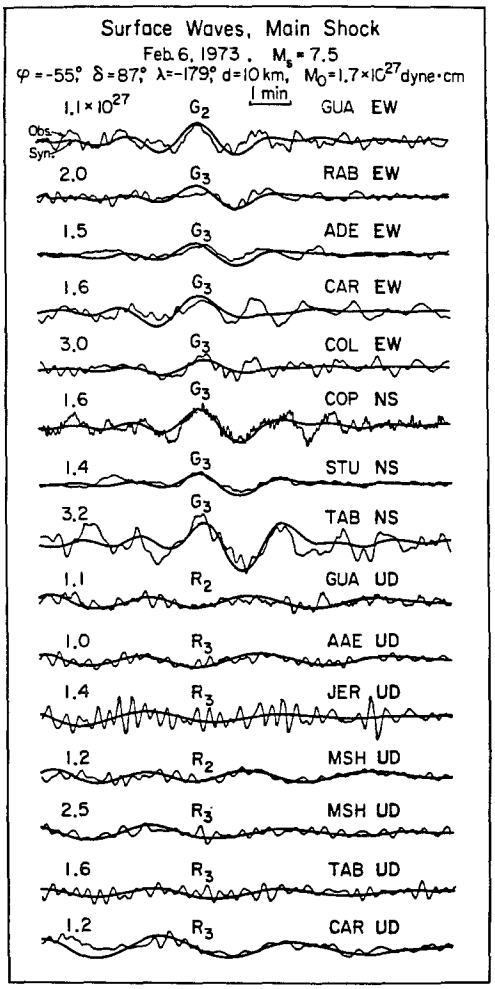

FIG. 5. The surface waves (G_2, G_3, R_2, and R_3) for the 6 February 1973 event. The solid thin traces are the observed seismograms and the thick traces are the synthetics computed for the body-wave source mechanism. The numbers attached to each trace give the seismic moment of the synthetic. The moment is determined to be 1.7×10^{27} dyne-cm.

$\times 10^{26}$ dyne-cm. Our preferred model (the solid thin traces in Figure 4) explains the waveforms better at stations COL, GUA, RAB, and ADE. Apparently, the finite source rupture may have complicated the waveforms.

Using the source parameters obtained from the body waves, we synthesize the G_2, G_3, R_2, and R_3 waves and compare them with the seismograms obtained at the WWSSN stations in Figure 5. The seismic moment determined from the surface waves is 1.7×10^{27} dyne-cm, which is about the same as the body-wave moment.

Hence, our preferred body-wave model represents a reasonable overall source process.

A major aftershock of the 1973 event. The largest (M_S = 5.9) aftershock occurred 24 hr after the main shock (M_S = 7.5). The event is located about 20 km west of Luhuo, and is slightly off the main surface trace of the Xianshuihe fault. A pure normal-fault mechanism striking N30°E, dipping 60°NW (or 30°SE) is found from the teleseismic synthetic *P* waves. Figure 6 illustrates the first-motion data, the observed *P* waves, and the preferred synthetic seismograms computed for our preferred model. The width of the trapezoidal source time function is determined to be 2.5 sec. The source depth is assumed to be 10 km. The seismic moment determined from nine teleseismic stations is 5.9×10^{24} dyne-cm.

The 1981 main shock. The 23 January 1981 earthquake is located near Daofu, which is close to the central portion of the Xianshuihe fault and caused a 44 km

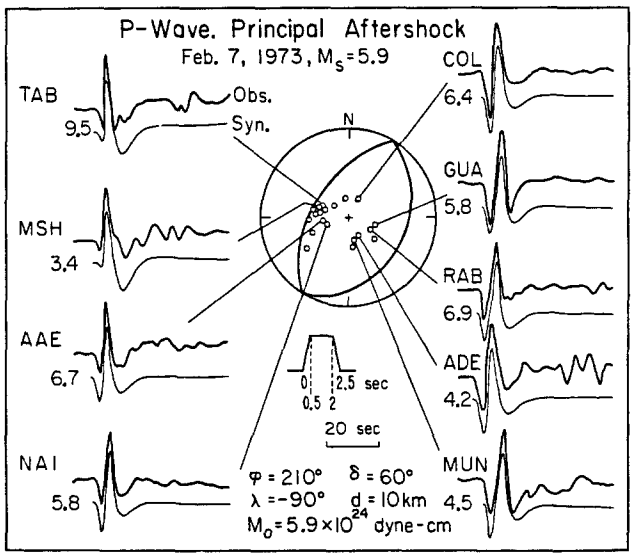

FIG. 6. The major aftershock (M_S = 5.9) of the 1973 event. The best-matched synthetics indicate a normal-fault mechanism [with strike = 210°, dip = 60° (NW), and slip = −90°], which is different from the left-lateral strike-slip mechanism of the main shock.

surface rupture along it (Yaoguo Zhang, personal communication, 1981). At the beginning of this study, only long-period surface and body waves recorded at SRO and ASRO stations are available. We inverted the Rayleigh- and Love-wave spectra at the period of 200 sec by using a moment tensor or a fault model (Kanamori and Given, 1981) and obtained a pure left-lateral strike-slip mechanism on a vertical fault striking N41°W with a seismic moment of 8.5×10^{26} dyne-cm. The amplitude and phase spectra are explained very well with this model (Figure 7). Our solution agrees very well with that obtained by Dziewonski and Woodhouse (1982). The *P* waveforms from this event show some complexity which can be explained by two equal-sized sources about 22 sec apart and having a total seismic moment of 1.3×10^{24} dyne-cm (Figure 8a). This value is slightly larger than the surface-wave moment, although the difference is considered insignificant. The separation of these two subevents determined for each station is given by a number at the *top-right corner*

of each seismogram shown in Figure 8a. The azimuthal variation of the time separation suggests that the second event is located at about 10 km to the southeast of the first one.

During the later stage of this study, the WWSSN data became available. As an independent check, we computed the synthetic waves using this source model and compared them with those observed at WWSSN stations (Figure 8b). Our source model can explain the WWSSN seismograms reasonably well.

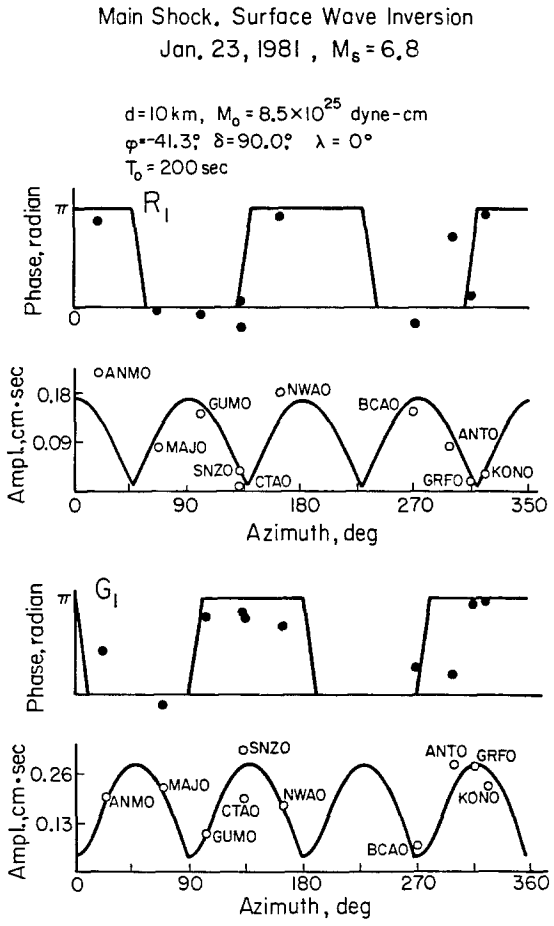

FIG. 7. The surface wave source parameters for the 23 January 1981 event. Both phase and amplitude spectra of G_1 and R_1 waves are used to obtain the source mechanism at the period of 200 sec. The moment is determined to be 8.5 × 10^{25} dyne-cm.

SUMMARY OF THE RESULTS AND DISCUSSION

(1) The largest 1973 event and the second largest 1981 event represent left-lateral strike-slip motion along the Xianshuihe fault. In the area from Luhuo to Ganzi (see Figure 1b), a relatively small event in 1967 and two aftershocks in 1967 and 1973, have a normal-fault mechanism with a strike nearly perpendicular to the strike of Xianshuihe fault. The strike-slip motion along the Xianshuihe fault associated with the larger events represent the major tectonic deformation in this area, the normal faulting being considered as a secondary phenomenon.

A simple mechanical model proposed by Molnar and Tapponnier (1975), and Tapponnier and Molnar (1977) can explain this regional tectonic structure. The Indian plate collides with the Eurasian plate with a convergence direction of about N70°E in the southwestern part of this area (see Figure 9). This collision caused extensive folding, active thrust faulting, and the remarkable bending of structure

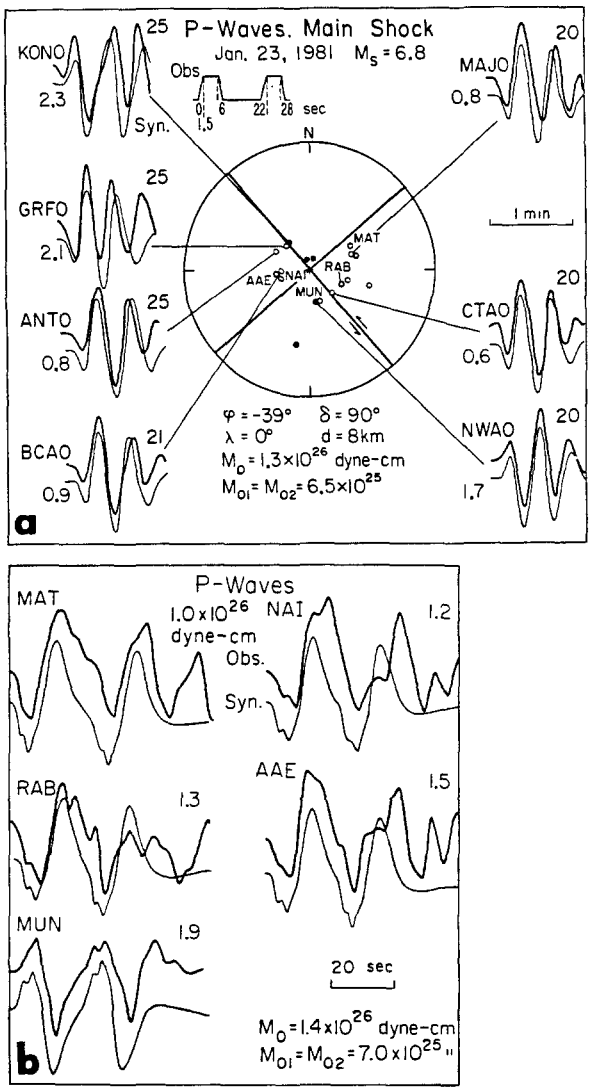

FIG. 8. (a) The observed and synthetic *P* seismograms for the 23 January 1981 earthquake. The best synthetics indicate a mechanism which consists of two strike-slip events. These two events have the same fault geometry and occurred about 22 sec apart as indicated in the source time history. The separation time of the two events at each station is indicated by the number written at the *top-right corner*. (b) The observed and synthetic *P* waves at WWSSN stations for the 1981 event.

lines in southwestern China. The Xianshuihe fault can be considered as a boundary between a highly deformed block to the southwest and a relatively undeformed block to the northeast. Under the regional compression, the southeastern deformed block tends to move out laterally along the Xianshuihe fault. The larger earthquakes such as the 1973 and the 1981 events represent this motion. This lateral motion

causes extensional stress in the deformed block to the northwest of the epicenters of these two large events, causing smaller normal-fault events. Another possible interpretation is that the extensional stress is a result of the en-echelon offset of the left-lateral Xianshuihe fault there (see Figure 1, a and b, and Figure 9). This en-echelon offset may have been caused by the bending force exerted on southwestern China by the India-Tibet collision.

(2) The *P*-waveform analysis of these earthquakes shows that the 1973 and 1981 events which occurred along the locked segment of the major fault have complex waveforms. This complexity is probably due to the irregular stress field along a very long fault. On the other hand, the 1967 event and the two aftershocks which occurred on the minor normal faults in this area have relatively simple waveforms.

(3) The source parameters of these five events are summarized in Table 3. The amount of dislocation D and the stress drop $\Delta\sigma$ are estimated with a rectangular fault geometry and an assumed rigidity of 3.0×10^{11} dyne/cm^2 using the formulas

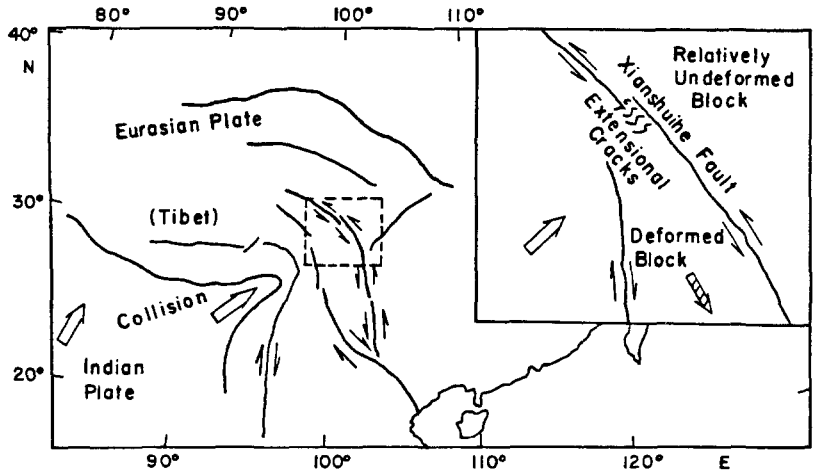

FIG. 9. A mechanical model to interpret the possible mechanisms for the Xianshuihe fault and the surrounding tectonic features.

summarized by Kanamori and Anderson (1975). The fault width W is assumed to be equal to the down-dip distance from the surface to the hypocenter. L_1 is the length of the surface break and L_2 the long axis of the aftershock area (Figure 10, b, d, and f) (data from the *Earthquake Catalogue of Sichuan Province, China*). L_3 is the rupture length estimated from the duration of the time function: $L_3 = v_r t_c$, where v_r is the assumed rupture velocity 3.5 km/sec, and t_c is the effective time function duration (t_c = 32 sec, 12 sec, and 2.5 sec for the 1973, 1981, and 1967 events, respectively). For the 1973 and 1981 events, L_1, L_2, and L_3 are nearly equal. By using L_1, D = 380 cm and $\Delta\sigma$ = 50 bar are obtained for the 1973 event, and D = 100 cm, $\Delta\sigma$ = 20 bar for the 1983 event. For the 1967 event, no evident surface rupture is reported. The length of the aftershock area L_2 is anomalously long (42 km). The values of D (150 cm) and $\Delta\sigma$ (35 bar) are computed here by using L_3 (9 km).

A similar discrepancy between L_3 and L_2 is found for the Haicheng earthquake (4 February 1975, M_S = 7.3). Cipar (1979) gave L_3 = 22 km, which is much smaller than L_2 (70 km) (Gu *et al.*, 1976).

TABLE 3
SOURCE PARAMETERS

Event	M_S	Depth (km)	Source Geometry			$M_0 \times 10^{24}$ (dyne-cm)	W (km)	L_1 (km)	L_2 (km)	L_3 (km)	D (cm)	$\Delta\sigma$ (bar)
			ϕ (°)	δ (°)	λ (°)							
30 August 1967	6.1	8	245	45	−70	45	11					
									42			
										9	150	35
Major aftershock	5.1	10	233	50	−90	2.2	13					
6 February 1973	7.5	10 (1, 2)	−55	87	−179	1800	15	90			380	50
		15 (3)	−70	80	−178				110			
										110		
Major aftershock	5.9	10	210	60	−90	5.9	12					
23 January 1981	6.8	10	−40	90	0	130	10	44			100	20
									46			
										42		

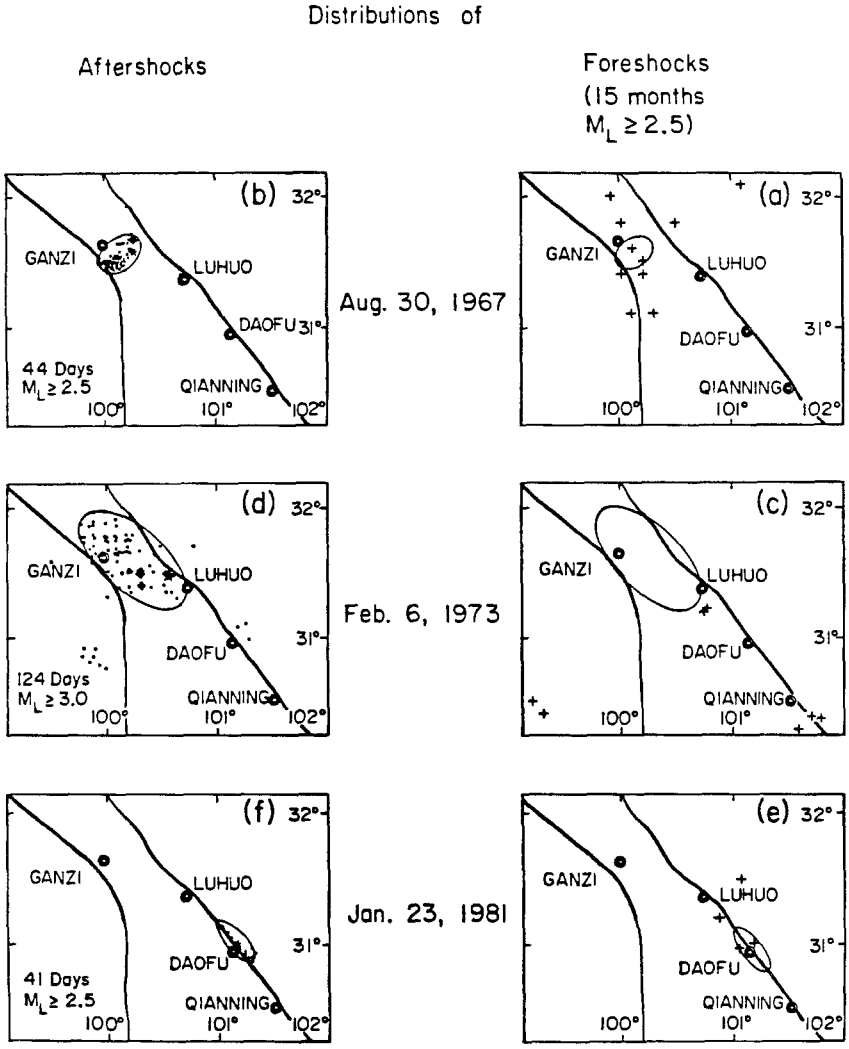

FIG. 10. The foreshocks and aftershocks distribution for the 1967, 1973, and 1981 events along the Xianshuihe fault.

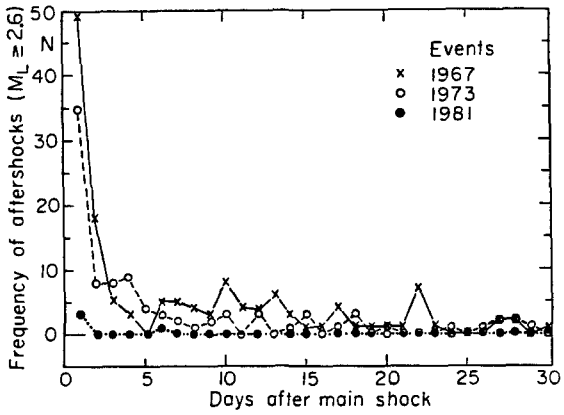

FIG. 11. The aftershock frequency curve for the 1967, 1973, and 1981 events.

Neither the 1967 Ganzi event nor the 1975 Haicheng event occurred along the trend of a major regional fault. It seems that these kinds of events have somewhat similar characteristics: (a) The aftershock area is anomalously large and probably does not represent the actual rupture zone. If this is the case it cannot be used to calculate the slip and stress drop. (b) The surface rupture is very short or not evident. (c) The values of D and $\Delta\sigma$ obtained by waveform analysis are more reasonable. The values of D and L estimated by this method are larger than those of the surface break. This discrepancy may be due to the dying out of the slip as it approaches the surface.

In fact, not only the aftershock area but also the number of aftershocks ($M_L \geqq 2.6$) of the 1967 event are larger than the 1973 and 1981 events despite its smaller magnitude (Figure 11). This result is in harmony with the conclusion of Gibowicz (1973) that events which occur on a less developed or a new fault are followed by more aftershocks than those which occur on a well-developed fault.

(4) Figure 10, a, c, and e, shows the seismic activity ($M_L \geqq 2.5$) during the 15 months before the 1967, 1973, and 1981 events, respectively. Before the 1967 event, a relatively large number of small events which may be called foreshocks occurred; the last foreshock occurred about 20 min (dt) before the main shock at about 14 km (dl) to the southwest of the main shock epicenter. Before the 1973 and the 1981 events, only a few events occurred. For the 1973 event, $dt = 98$ days, $dl = 151$ km; for the 1983 event, $dt = 91$ days, $dl = 36$ km; i.e., during more than 90 days before these two events, there was no period of seismic quiescence in the epicentral area. For the 1967 event, from 1966 to the origin time of the main event, and especially just before it, the residents in the epicentral area felt numerous shocks, and the Ganzi Weather Station recorded them. In contrast, people did not feel any shocks in the epicentral area before the 1973 event, and only six very small events ($M_L \leqq 1.5$) were recorded in the last 3 months before the 1981 event, despite the fact that the Daofu Seismic Station equipped with high-gain seismographs is very close to the main shock epicenter (Figures 1b and 10e). It appears that events which do not occur on major faults are more likely to be preceded by foreshocks.

Conclusions

The source parameters determined from the waveform analyses for the 1967, 1973, and 1981 earthquakes along the Xianshuihe fault indicate that this active fault is dominated by about N40°W striking left-lateral motion with the compressional axis oriented about NEE, which is close to the trend of the India-Tibet collision to the southwest. Normal faulting is also common for smaller size earthquakes near the northwestern end of the Xianshuihe fault. One possible interpretation for these complexities is that the Xianshuihe fault is a contact zone between a relatively undeformed block to the northeast and a severely deformed block to the southwest. The left-lateral motion along the fault is the result of the southwestward relative motion of the deformed block. The normal-fault events near Ganzi may be a result of the tensional stress caused by the left-stepping offset of the Xianshuihe fault near Luhuo, as well as by the left-lateral motion along the Xianshuihe fault to the southwest.

The P waveforms of the 1973 and 1981 events which occurred along the locked segment of well-developed old major fault are more complex than those of the 1967 event which occurred on a less developed fault.

It seems that in this area, the events which are not on the major fault, such as the 1967 Ganzi event, are more likely to be preceded by foreshocks and followed by

numerous aftershocks, compared with those on the major fault, such as the 1973 Luhuo and 1983 Daofu events.

Acknowledgments

We wish to give special thanks to Professor Clarence Allen for very kindly supporting this project, reading the manuscript, and making many valuable suggestions. The first author is also grateful to Jeff Given, Ed Corbett, Fumiko Tajima, Gladys Engen, Jeanne Sauber, and Larry Ruff for their help in the use of the computer and the SRO data tape. Research supported by the Division of Earth Sciences, National Science Foundation, NSF Grant EAR-811-6023, and the U.S. Geological Survey Contract 14-08-0001-19265.

References

Cipar, J. (1979). Source processes of the Haicheng, China earthquake from observations of *P* and *S* waves, *Bull. Seism. Soc. Am.* **69,** 1903–1916.

Dziewonski, A. M. and J. H. Woodhouse (1982). An experiment in systematic study of global seismicity: centroid-moment tensor solutions for 201 moderate and large earthquakes of 1981, *J. Geophys. Res.* (in press).

Gibowicz, S. J. (1973). Stress drop and aftershocks, *Bull. Seism. Soc. Am.* **63,** 1433–1446.

Gu, H., *et al.* (1976). Focal mechanism of Haicheng, Liaoning province, earthquake of February 4, 1975, *Acta Geophys. Sin.* **19,** 270–284 (in Chinese).

Heim, A. (1934). Earthquake region of Taofu, *Bull. Geol. Soc. Am.* **45,** 1035–1050.

Kan, R., *et al.* (1977). Present tectonic stress field and its relation to the characteristics of recent tectonic activity in southwestern China, *Acta Geophys. Sin.* **20,** 96–108 (in Chinese).

Kanamori, H. and D. L. Anderson (1975). Theoretical basis of some empirical relations in seismology, *Bull. Seism. Soc. Am.* **65,** 1073–1095.

Kanamori, H. and G. S. Stewart (1976). Mode of the strain release along the Gibbs fracture zone, Mid-Atlantic Ridge, *Phys. Earth Planet. Interiors* **11,** 312–332.

Kanamori, H. and J. W. Given (1981). Use of long-period surface waves for the fast determination of earthquake source parameters, *Phys. Earth Planet. Interiors* **27,** 8–31.

Lee, S. P. (1948). Tectonic relation of seismic activity near Kangting, east Sikang, *Bull. Geophys. China* **1,** 43–50.

Molnar, P. and P. Tapponnier (1975). Cenozoic tectonics of Asia: effects of a continental collision, *Science* **189, 4201,** 419–426.

Tang, R., *et al.* (1976). A preliminary study on the characteristics of the ground fractures during the Luhuo $M = 7.9$ earthquake, 1973 and the origin of the earthquake, *Acta Geophys. Sin.* **19,** 18–27.

Tapponnier, P. and P. Molnar (1977). Active faulting and tectonics in China, *J. Geophys. Res.* **82,** 2905–2930.

Seismological Laboratory
California Institute of Technology
Pasadena, California 91125
Contribution No. 3784

Manuscript received 12 July 1982